

# tRNA selection and kinetic proofreading in translation

Scott C Blanchard<sup>1,2</sup>, Ruben L Gonzalez Jr<sup>2,3</sup>, Harold D Kim<sup>1,3</sup>, Steven Chu<sup>1</sup> & Joseph D Puglisi<sup>2</sup>

**Using single-molecule methods we observed the stepwise movement of aminoacyl-tRNA (aa-tRNA) into the ribosome during selection and kinetic proofreading using single-molecule fluorescence resonance energy transfer (smFRET). Intermediate states in the pathway of tRNA delivery were observed using antibiotics and nonhydrolyzable GTP analogs. We identified three unambiguous FRET states corresponding to initial codon recognition, GTPase-activated and fully accommodated states. The antibiotic tetracycline blocks progression of aa-tRNA from the initial codon recognition state, whereas cleavage of the sarcin-ricin loop impedes progression from the GTPase-activated state. Our data support a model in which ribosomal recognition of correct codon-anticodon pairs drives rotational movement of the incoming complex of EF-Tu-GTP-aa-tRNA toward peptidyl-tRNA during selection on the ribosome. We propose a mechanistic model of initial selection and proofreading.**

mRNA-directed protein synthesis is carried out by the ribosome, a two-subunit RNA-protein enzyme that catalyzes repetitive selection of the aa-tRNA corresponding to a specific three-base codon sequence within mRNA. Three roughly parallel binding sites for tRNA have been identified on both the large (50S) and small (30S) subunits of the *Escherichia coli* ribosome, called the aminoacyl (A), peptidyl (P) and exit (E) sites<sup>1</sup>. Peptidyl-tRNA preferentially binds at the P site, whereas aa-tRNAs are selected in an empty A site. aa-tRNAs are delivered to the ribosome as a 'ternary complex' with the GTPase elongation factor-Tu (EF-Tu) bound to GTP<sup>2</sup>. EF-Tu increases both the rate and fidelity of tRNA selection<sup>3,4</sup>.

Detailed kinetic information about EF-Tu-mediated aa-tRNA selection at the A site of the ribosome has chiefly been explained through a series of pioneering fluorescence and biochemical experiments<sup>5,6</sup>. Ternary complex (EF-Tu-GTP-aa-tRNA) entering the ribosome initially binds the 50S subunit through protein-protein interactions with the tetrameric protein L7/L12 (refs. 7,8). After binding to L7/L12 takes place, the mRNA codon and tRNA anticodon pair within the A site of the 30S subunit. The interaction of cognate aa-tRNA with the ribosome enhances the rate of GTP hydrolysis by EF-Tu by as much as  $5 \times 10^4$  (ref. 9). After hydrolysis, EF-Tu-GDP adopts a conformation with a low affinity for aa-tRNA<sup>10</sup>, allowing the 3' end of the tRNA to accommodate within the peptidyl transferase center (PTC) of the 50S subunit. There, a peptide bond is formed between the amino acids of the adjacent P- and A-site tRNAs. Several antibiotics inhibit the distinct steps of the aa-tRNA selection process<sup>5,6,11</sup>.

*In vivo*, 5–20 aa-tRNAs are delivered to the ribosome per second, with an average error frequency of  $5 \times 10^{-3}$  (ref. 12). The fidelity of translation cannot be explained by the differences in the free energy of binding between the mRNA codon and the anticodon of the cognate (at least two matched base pairs), near-cognate (at least one base mismatch) and noncognate tRNA<sup>13</sup>. To resolve this dilemma, a kinetic

proofreading model was proposed in which an initial selection step is isolated from a second proofreading step by irreversible phosphate hydrolysis<sup>14,15</sup>. In this model, preferential selection of cognate aa-tRNAs was thought to arise from rapid dissociation of near-cognate and noncognate tRNAs before and after GTP hydrolysis. This two-step tRNA selection process has been verified<sup>6,16,17</sup>. However, it was later shown that the ribosome also actively recognizes cognate aa-tRNA selection through shape discrimination of the codon-anticodon duplex<sup>18–20</sup> and that both initial selection and proofreading steps operate through 'induced-fit' mechanisms<sup>17,21</sup>.

The molecular mechanism linking codon recognition to stimulated GTP hydrolysis by EF-Tu is essential to the understanding of fidelity in translation<sup>1</sup>. Hydrolysis can only occur if an allosteric signal from the codon-anticodon recognition site on the 30S subunit is transmitted to the GTPase domain of EF-Tu ~80 Å away, through changes either in the conformation of tRNA or in the subunit interface<sup>17,22,23</sup>. The GTPase activation center of the ribosome is located within the 50S subunit and involves conserved RNA elements, such as the sarcin-ricin loop (SRL) and proteins L7/L12, L10 and L11 (ref. 10). A mechanistic model has recently been proposed to explain codon-dependent GTPase activation of EF-Tu based on a cryo-EM structure of the ribosome trapped in an intermediate state in aa-tRNA selection<sup>24</sup>. These data suggest that distortions in aa-tRNA structure and position with respect to EF-Tu trigger codon recognition and subsequent GTPase activation and hydrolysis. Structural evidence also suggests that interaction of cognate tRNA with the 30S subunit induces domain movements that may be related to GTPase activation and accommodation steps<sup>21</sup>.

To understand the dynamic processes that lead to translational fidelity, we carried out a single-molecule fluorescence study of EF-Tu-mediated aa-tRNA selection on the ribosome. Using fluorescently labeled tRNA molecules, real-time observation of aa-tRNA selection

<sup>1</sup>Department of Physics and Applied Physics, Stanford University, Stanford, California 94305-4060, USA. <sup>2</sup>Department of Structural Biology, Stanford University School of Medicine, Stanford, California 94305-5126, USA. <sup>3</sup>These authors contributed equally to this work. Correspondence should be addressed to S.C. (schu@stanford.edu) or J.D.P. (puglisi@stanford.edu).

showed progressively increasing FRET between tRNAs in adjacent binding sites on the ribosome. Intermediate states in the selection process were further identified using antibiotic inhibitors of tRNA selection, nonhydrolyzable GTP analogs, and enzymatically and chemically altered ribosome complexes. We identified a new codon recognition state in the aa-tRNA selection process and provide evidence that the SRL<sup>10</sup> is directly involved in GTP hydrolysis by EF-Tu after initial selection has occurred. On the basis of these data, we present a new model for ribosomal allostery, in which interaction of cognate tRNA with the mRNA codon on the 30S subunit leads to rotational movement of the ternary complex toward the P site to allow productive interaction of EF-Tu with the SRL and subsequent GTP hydrolysis. Comparison of cognate and near-cognate aa-tRNA selection using our smFRET data confirms that the overall fidelity is established by initial selection and proofreading.

## RESULTS

### smFRET analysis of tRNA delivery

In this study, *E. coli* ribosomes were initiated *in vitro* with fMet-tRNA<sup>fMet</sup> in the P site fluorescently labeled with cyanin 3 (Cy3) at the 4-thiouridine (s<sup>4</sup>U8) residue<sup>25</sup>. The ribosomes were then tethered to a streptavidin-coated surface via interactions with 5'-biotinylated mRNA<sup>26</sup>. Stopped-flow delivery of EF-Tu-GTP-Phe-tRNA<sup>Phe</sup> to surface-immobilized particles (labeled with Cy5 at the 3-(3-amino-3-carboxypropyl)uridine (acp<sup>3</sup>U47) residue<sup>27</sup>) generated a rapidly evolving smFRET signal<sup>26</sup>. Numerous individual ribosomes were observed simultaneously, and single-molecule time traces (Fig. 1) were superimposed and plotted as a contour plot to generate the time evolution of population FRET<sup>26</sup> (Fig. 2). To eliminate blurring of data owing to asynchronous initial binding of ternary complex to the ribosome, smFRET time traces have been 'postsynchronized' to the first FRET signal above a minimum threshold ( $\geq 0.25$ ).

The majority of smFRET time traces show a rapid evolution from low to high FRET (mean value  $\sim 0.75$ , Supplementary Fig. 1 online), followed by dynamic fluctuations to intermediate FRET. Stable occupancy of the 0.75 FRET state results from complete accommodation of the Phe-tRNA<sup>Phe</sup> into the A site of the ribosome and peptide bond formation<sup>26</sup>. Fluctuations in FRET after accommodation correspond to tRNA dynamics on the ribosome and photophysical 'blinking' events<sup>26</sup>. The apparent rate for initial binding, as determined by the arrival times of initial FRET ( $\geq 0.25$ ) at a concentration of 7.5 nM ternary complex, is  $0.77 \text{ s}^{-1}$  (Supplementary Fig. 2 online), in agreement with a previously reported bimolecular rate constant of  $\sim 7 \times 10^7 \text{ M}^{-1}\text{s}^{-1}$  (ref. 9). The time required for FRET to evolve from initial binding (FRET  $\geq 0.25$ ) to complete accommodation

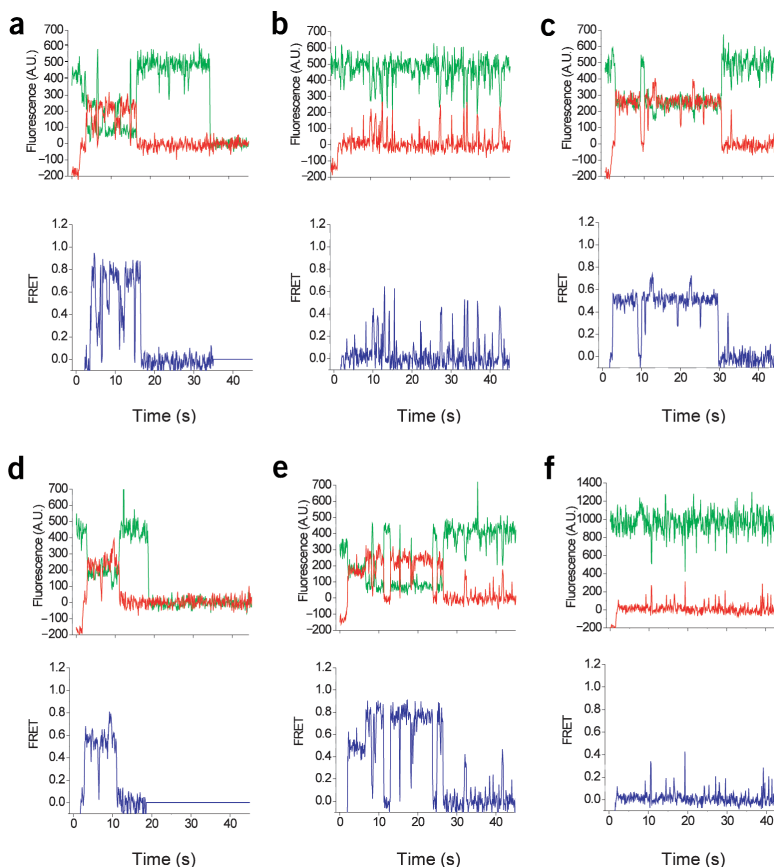


**Figure 1** Single-molecule fluorescence intensity and FRET time traces. Each panel shows representative fluorescence data from single molecules after stopped-flow delivery of EF-Tu-GTP-Phe-tRNA<sup>Phe</sup>(Cy5-acp<sup>3</sup>U47) to surface-immobilized ribosome complexes carrying fMet-tRNA<sup>fMet</sup>(Cy3-s<sup>4</sup>U8) in the P site. Weak, direct excitation of EF-Tu-GTP-Phe-tRNA<sup>Phe</sup>(Cy5-acp<sup>3</sup>U47) in solution by 532-nm illumination led to change in the baseline Cy5 fluorescence upon mixing. The time trajectory of smFRET data provides information about tRNA dynamics on individual ribosome complexes. Each panel shows Cy3 and Cy5 fluorescence intensity (top) and FRET (bottom) for representative molecules from each experiment described in the text. (a) Cognate aa-tRNA delivery. (b) Cognate aa-tRNA delivery in the presence of 100  $\mu\text{M}$  tetracycline. (c) Cognate aa-tRNA delivery in the presence of the nonhydrolyzable GTP analog, GDPNP. (d) Cognate aa-tRNA delivery in the presence of 200  $\mu\text{M}$  kirromycin. (e) Cognate aa-tRNA delivery to ribosome complexes cleaved at the SRL. (f) Near-cognate aa-tRNA delivery. Cy3 (green) and Cy5 (red) fluorescence intensity is plotted in arbitrary units (A.U.) as recorded by the CCD. FRET, characterized by anticorrelated changes in Cy3 and Cy5 fluorescence, is calculated from the fluorescence intensity ( $I$ ) according to the equation  $I_{\text{Cy5}} / (I_{\text{Cy3}} + I_{\text{Cy5}})$ . smFRET data also include photophysical phenomena such as photobleaching and 'blinking' events observed as spontaneous loss of Cy3 and/or Cy5 fluorescence<sup>26</sup> as well as information about dissociation of tRNA from the ribosome. Blinking is observed as an intermittent loss of Cy5 fluorescence (FRET = 0), where the lifetime of the nonfluorescent state is  $\sim 1 \text{ s}$ .

(FRET = 0.75) is  $\sim 93 \text{ ms}$  (Supplementary Fig. 3 online), also consistent with previous studies<sup>9</sup>.

To help identify intermediate FRET states in tRNA selection, known inhibitors of A-site tRNA binding were incorporated into smFRET experiments. The antibiotic tetracycline inhibits A-site tRNA delivery to the *E. coli* ribosome<sup>28</sup>. In the presence of 100  $\mu\text{M}$  tetracycline, selection of EF-Tu-GTP-Phe-tRNA<sup>Phe</sup>(Cy5-acp<sup>3</sup>U47) was inhibited (Fig. 1b). smFRET traces show that low FRET (mean value  $\sim 0.35$ , Supplementary Fig. 1 online) states are transiently sampled. Rare, transient states with higher FRET values ( $\geq 0.5$  FRET) were also observed. In the presence of 100  $\mu\text{M}$  tetracycline and the nonhydrolyzable GTP analog, GDPNP, FRET states  $> 0.70$  were no longer observed (data not shown). The time delay between FRET events

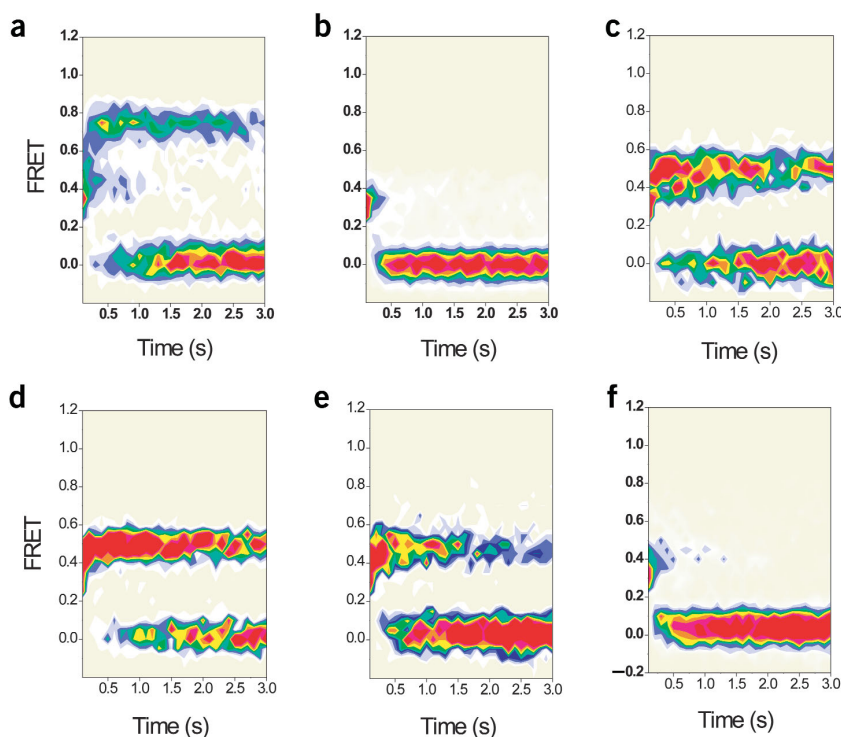


**Figure 2** Contour plots of the time evolution of population FRET. Each plot was generated by superimposing the individual smFRET time traces obtained in stopped-flow delivery experiments (as in Fig. 1). Data were ‘postsynchronized’ to the first observation of FRET  $\geq 0.25$ . Contours are plotted from tan (lowest population) to red (highest population). Molecules in the FRET = 0 state arise from photobleaching and blinking of Cy5 as well as the dissociation of tRNA from the ribosome.

( $1.45 \pm 0.02$  s, Supplementary Fig. 4 online) is comparable to the FRET arrival time observed in uninhibited tRNA delivery (1.29 s) and in the presence of tetracycline (1.8 s). Hence, each event is interpreted as an independent attempt of the aa-tRNA to enter the ribosome. Rather than disrupting initial binding and codon recognition on the ribosome, tetracycline inhibits subsequent events required for aa-tRNA selection. The contour plot showing the time evolution of population FRET (Fig. 2b) reveals that, in the presence of tetracycline, most accommodating aa-tRNAs are rejected from the 0.35 FRET state, where the lifetime of this state is  $177 \pm 4$  ms (Supplementary Fig. 4 online).

aa-tRNA selection is efficiently stalled using GDPNP<sup>9</sup>. EF-Tu-GDPNP-Phe-tRNA<sup>Phe</sup>(Cy5-acp<sup>3</sup>U47) binds to the ribosome, rapidly transits through the 0.35 FRET state and stabilizes at a FRET value of 0.5 (Fig. 2c and Supplementary Fig. 1 online).

The lifetime of GDPNP-stalled complexes,  $8.3$  s  $\pm$   $0.24$  (Supplementary Fig. 5 online), is comparable to that in previous reports<sup>17</sup>. The lifetime is  $\sim 45$ -fold longer than that of the 0.35 FRET state observed in the presence of tetracycline (Fig. 2b,c). These data show that the movement of the complex from 0.35 to 0.5 FRET states generates additional stabilizing contacts between the ternary complex and the ribosome that form before GTP hydrolysis. Individual time traces show that the 0.5 FRET state is punctuated by short-lived fluctuations to both higher ( $>0.7$ ) and lower ( $\sim 0.35$ ) FRET states occurring at about one per second (Fig. 1c).

aa-tRNA selection can be stalled after GTP hydrolysis using the antibiotic kirromycin<sup>29</sup>. Kirromycin binds directly to EF-Tu-GTP-aa-tRNA at the interface of domains, inhibiting the structural transition of EF-Tu to the GDP-bound conformation<sup>30,31</sup>. Delivery of EF-Tu-

GTP-Phe-tRNA<sup>Phe</sup>(Cy5-acp<sup>3</sup>U47) to the ribosome in the presence of 200  $\mu$ M kirromycin stalled selection at a 0.5 FRET state (Fig. 2d and Supplementary Fig. 1 online) after progression through 0.35 FRET similar to that of the GDPNP-stalled complex (Fig. 2c). The kirromycin-stalled complex was likewise kinetically stable, and fluctuations to both high and low FRET were observed. The GDPNP- and kirromycin-stalled tRNA configurations are equivalent to the A/T state described elsewhere<sup>32</sup>.

### Role of SRL in tRNA selection

Cleavage of a single phosphodiester bond within the large subunit in the universally conserved SRL (nucleotides 2654–2666, *E. coli*) by the plant toxin  $\alpha$ -sarcin inactivates the ribosome by inhibiting tRNA delivery mediated by EF-Tu and translocation mediated by EF-G<sup>33</sup>. The SRL also has an important yet poorly understood role in promoting fidelity in tRNA selection<sup>34</sup>. Ribosomes bearing a G2661C mutation are hyperaccurate in tRNA selection and show diminished levels of GTP hydrolysis<sup>35</sup>. EF-Tu-GDPNP-aa-tRNA footprints the SRL, and cryo-EM structures show the SRL interacting directly with EF-Tu near the GTP-binding site<sup>32,36,37</sup>.

To test the role of the SRL in tRNA selection, ribosomes were cleaved with the  $\alpha$ -sarcin homolog, restrictocin, before sur-

face immobilization (Supplementary Fig. 6 online). Ternary complex delivered to cleaved ribosomes rapidly generated a FRET state with a mean FRET value of 0.5, where the aa-tRNA is stalled before complete accommodation at the A site (Fig. 2e and Supplementary Fig. 1 online). The rate of transition from FRET  $\geq 0.25$  to the 0.75 FRET state is decreased by  $\sim 13$ -fold compared with unmodified ribosomes (Supplementary Fig. 7 online), whereas the rate of arrival to the initial 0.35 FRET state is unaffected (Supplementary Fig. 2 online). Individual time traces reveal the effect of restrictocin cleavage. Most ribosomes ( $\sim 77\%$ ) rapidly reached the 0.5 FRET state and were stalled there, with transient fluctuations to the 0.75 FRET state, as in the GDPNP- and kirromycin-stalled complexes. Approximately 15% of the tRNAs were directly observed to progress into the 0.75 FRET state after an extended delay at 0.5 FRET.

### Fidelity of near-cognate tRNA selection

Ribosomes programmed with a near-cognate codon (CUU instead of cognate UUU) rarely incorporated aa-tRNAs (Fig. 1f). The time evolution of population FRET (Fig. 2f) reveals that near-cognate aa-tRNAs transiently occupy the 0.35 FRET state and make much rarer, short-lived transitions to higher FRET states. Thus, an important selection step must take place that prevents most near-cognate aa-tRNAs from progressing beyond the 0.35 FRET state (compare Fig. 2a,f). Programming the A site with a noncognate lysine codon (AAA versus UUU) effectively eliminated tRNA sampling of the codon recognition state (0.35 FRET) on the time scale of our observations (data not shown).

To compare quantitatively the fidelity of cognate and near-cognate tRNA selection, we made corrections to the single-molecule data. Of

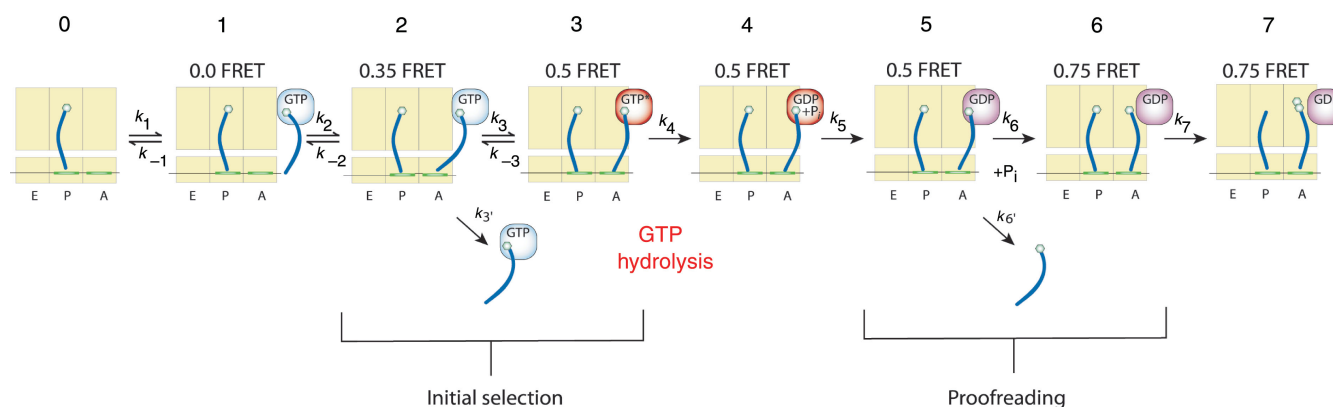


**Figure 3** A revised model for tRNA selection at the A site inferred from smFRET data (based on the scheme described in ref. 17) schematizing EF-Tu-regulated movements of aa-tRNA into the accommodated state (0.75 FRET). Small and large subunits of the ribosome are yellow. E, P and A sites are adjacent rectangles. tRNAs (blue) are shown attached to amino acids (green) corresponding to the mRNA codons in P and A sites of the small subunit. EF-Tu is in three colors corresponding to initial binding and codon recognition states (light blue), the GTPase-activated state, before and after GTP hydrolysis (red) and after conformational change to the GDP-bound form (purple). Step 1 ( $k_1 / k_{-1}$ ): initial binding is mediated by the interaction of EF-Tu-GTP-aa-tRNA with ribosomal protein L7/L12 (0 FRET). Step 2 ( $k_2 / k_{-2}$ ): contact is made between the anticodon of tRNA and the mRNA codon within the small subunit decoding site (codon recognition), generating a fixed orientation of EF-Tu-GTP-aa-tRNA with respect to the P-site tRNA (0.35 FRET). Step 3 ( $k_3 / k_{-3}$ ): productive codon recognition triggers a folding reaction between EF-Tu-GTP-aa-tRNA and the ribosome that moves aa-tRNA closer to the P site into a stabilized GTPase-activated state (0.5 FRET). Step 4 ( $k_4$ ): GTP hydrolysis is triggered by the interaction of EF-Tu with the SRL. Step 5 ( $k_5$ ): EF-Tu changes conformation from the GTP- to GDP-bound form. Step 6 ( $k_6$ ): aa-tRNA is released from EF-Tu to accommodate at the PTC. Step 7 ( $k_7$ ): peptide bond formation. In the proofreading steps of translation, aa-tRNA may dissociate from the ribosome through the pathways described by the rate constants  $k_3$  and  $k_6$ . All rate constants, where measured, are described in the text. Otherwise, rate constants are as reported in ref. 17.

116 molecules analyzed in cognate aa-tRNA delivery, ~16% of the ribosomes observed sample nonzero FRET but did not advance past the 0.5 state. This subpopulation of ribosomes showed an average of 2.5 unsuccessful attempts at tRNA selection per ribosome over the observation period, whereas the remaining 84% (97 molecules) reached a stable 0.75 FRET state, with an average of 0.24 failed attempts per ribosome before reaching this state. This marked difference in the two populations was used to identify and omit less active ribosomes from fidelity calculations.

Near-cognate and cognate aa-tRNAs differ markedly in the observed branching ratio exiting the 0.35 FRET state. Near-cognate aa-tRNAs preferentially dissociated from the ribosome; only 35 of 161 events (22%) advanced to the 0.5 FRET state. By contrast, 40 of 50 cognate events (80%) exited the 0.35 FRET state to higher FRET states. Thus, we observed a 3.6-fold (0.80/0.22) difference in the selection of cognate versus near-cognate aa-tRNAs to advance past the 0.35 FRET state during selection.

The ratio of preferential selection at the FRET = 0.35→0.5 step of cognate over near-cognate aa-tRNA is actually better than 3.6:1. By accounting for missed events (Supplementary Methods online and Supplementary Table 1 online), we calculate that the selection ratio of cognate versus near-cognate data sets is 5.9:1.

The overall error frequency of our ribosomes was calculated by counting the number of events in which the aa-tRNA was fully accommodated (stable 0.75 FRET state) and dividing by the total number of FRET events. The ratio of these values (near-cognate versus cognate) is  $\sim 7.1 \times 10^{-3}$  (Supplementary Methods online and Supplementary Table 1 online). Thus, to account for the difference between the overall fidelity and initial selection at the 0.35 FRET state, the proofreading step after GTP hydrolysis is estimated to have an error rate of 0.042, yielding a selection ratio of  $\sim 24:1$ . Thus, under our present conditions,  $\sim 80\%$  of the observed fidelity in tRNA selection is obtained in the proofreading step after GTP hydrolysis.

We further analyzed the tRNA selection process by examining the dynamics of GDPNP-stalled complexes. The population of the 0.35 FRET state before transitions to the 0 or 0.5 FRET state is described by a single-exponential decay with a lifetime ( $\tau$ ) of  $55 \pm 6$  ms (Supplementary Fig. 8 online). Because the 0.5 FRET state is very stable ( $\tau = 8.3$  s), the reverse rate  $k_{0.5 \rightarrow 0.35}$  can be ignored in relation to the rates  $k_{0.35 \rightarrow 0}$  and  $k_{0.35 \rightarrow 0.5}$ , and therefore,  $\tau \approx (k_{0.35 \rightarrow 0} + k_{0.35 \rightarrow 0.5})^{-1}$ . The values of  $k_{0.35 \rightarrow 0}$  and  $k_{0.35 \rightarrow 0.5}$  for cognate tRNA are determined by comparing the fraction of transitions from FRET = 0.35→0 in relation to FRET = 0.35→0.5. We find  $k_{0.35 \rightarrow 0.5} \approx 12$  s $^{-1}$  and  $k_{0.35 \rightarrow 0} \approx 6.4$  s $^{-1}$  for cognate tRNA. A similar analysis for near-cognate tRNA (Supplementary Fig. 9 online and Supplementary Table 1 online) leads to estimated rates of  $k_{0.35 \rightarrow 0.5} \approx 2.0$  s $^{-1}$  and  $k_{0.35 \rightarrow 0} \approx 16$  s $^{-1}$ . The rates  $k_{0.35 \rightarrow 0} = 5.6$  s $^{-1}$  and 8.5 s $^{-1}$  (for cognate and near-cognate aa-tRNAs, respectively) in the presence of tetracycline are in approximate agreement with the rates obtained here. Thus, it seems that tetracycline does not interfere with the dissociation rate  $k_{0.35 \rightarrow 0}$  but prevents the formation of contacts with the ribosome that stabilize the 0.5 FRET state. We estimate that all of our rates may be uncertain by as much as  $\sim 50\%$  because of uncertainties in the correction for the missing events.

### A revised model of tRNA selection

We summarize here the FRET states observed during tRNA delivery (Fig. 3) in a model that augments the scheme proposed elsewhere<sup>6,17</sup>. In state 1 (0 FRET, initial binding), EF-Tu interacts with L7/L12. Transient FRET signals were not observed upon delivery of ternary complexes to ribosome complexes programmed with a noncognate codon (AAA). The EF-Tu-GTP-aa-tRNA-L7/L12 interaction has a short lifetime ( $\sim 40$  ms) (ref. 38), and the distance between the accommodating tRNA and P-site tRNA is too great to generate a FRET signal  $\geq 0.25$ . This initial binding state corresponds to the state immediately after initial binding in the scheme proposed elsewhere<sup>6,17</sup>. In state 2 (0.35 FRET, codon recognition state), both cognate and near-cognate

ternary complex interact with mRNA on the 30S subunit. We believe that this state, not identified in earlier work, results from codon-anticodon recognition on the 30S subunit. The state transition from 0.35 FRET to 0.5 FRET is identified as the selection step at which both cognate and near-cognate aa-tRNAs can be rejected. The ratio of cognate to near-cognate tRNAs that advance to higher FRET states is 5.9:1. tRNA selection is primarily blocked at the 0.35 FRET state by the antibiotic tetracycline. Our finding that tetracycline blocks tRNA selection after codon recognition is also consistent with recent proposals based on X-ray crystallography<sup>39</sup>. Rare, transient excursions to higher FRET states could explain previous observations of slow GTP hydrolysis occurring in the presence of tetracycline<sup>40</sup>. In state 3 (0.5 FRET, pre-hydrolysis GTPase-activated state), initial selection of aa-tRNA is complete and ternary complex has formed, stabilizing contacts with the ribosome. Delivery of GDPNP-bound ternary complex produces a long-lived 0.5 FRET state. After reaching this state, the initial selection process is over. Once the 0.5 FRET state has been attained, GTPase hydrolysis can occur. We identify state 3 with that assigned by others as the state between codon recognition and GTPase activation<sup>5,6</sup>. In state 3, the GTPase activity of EF-Tu is stimulated and GTP is hydrolyzed. We observe a difference in the rate at which cognate and near-cognate aa-tRNA transition between states 2 and 3, whereas the codon recognition steps of previous tRNA selection schemes do not show a difference in the two forward rates<sup>6,17</sup>. In state 4 (0.5 FRET, post-hydrolysis GTPase-activated state), GTP hydrolysis has occurred. Comparison of GDPNP- and kirromycin-stalled data shows that our FRET probes cannot resolve the steps before and after hydrolysis. The transition of EF-Tu to the GDP-bound conformation, which is blocked by kirromycin, is expected to change the interaction between EF-Tu and aa-tRNA, the SRL and other components of the large subunit. In state 5 (0.5 FRET, pre-accommodation state), inorganic phosphate has been released from the EF-Tu-GDP-aa-tRNA complex, and EF-Tu has changed conformation to the GDP-bound form. In state 6 (0.75 FRET, accommodated state), the 3' end of aa-tRNA has accommodated at the PTC. The time required to pass from the 0.5 FRET state to the 0.75 FRET state is used to test the stability of aa-tRNA binding to the ribosome and is the second proofreading step in tRNA selection. In this accommodation step (defined here as the transition between 0.5 and 0.75 FRET states), cognate aa-tRNA is preferentially incorporated at the PTC over near-cognate aa-tRNA by a ratio of 24:1. In state 7 (0.75 FRET, post-peptide bond formation accommodated state), rapid peptide bond formation has taken place upon docking of aa-tRNA at the PTC<sup>17,26</sup>.

## DISCUSSION

Using single-molecule fluorescence, we have observed novel, transient states in the process of tRNA selection. Both the 0.35 FRET state and its transition to the 0.5 FRET state are novel codon recognition events. The 0.35 FRET state corresponds to an initial codon recognition state that is structurally and kinetically distinct from the 0.5 FRET state at which GTP hydrolysis occurs. Cognate aa-tRNA dissociates from the 0.35 FRET state at a rate of  $\sim 6.4 \text{ s}^{-1}$  (at 15 mM  $\text{Mg}^{2+}$ ), whereas the dissociation rate from the 0.5 FRET state is  $\sim 0.12 \text{ s}^{-1}$ . This latter rate is similar to the rate of EF-Tu-GDPNP-aa-tRNA dissociation,  $k_{-2}$ , measured by other groups after codon recognition and is considered part of their initial selection process<sup>6,17</sup>. Our work shows that the formation of the stable 0.5 FRET state occurs after initial selection is completed.

During the early stages of initial selection, the ternary complex is weakly bound to the ribosome by direct interaction of EF-Tu with ribosomal protein L7/L12 and by interaction of tRNA with mRNA and

components of the 30S subunit at codon recognition<sup>9,19</sup>. Residues A1492, A1493, G530 and ribosomal protein S12 likely mediate early events in shape-specific recognition of the codon-anticodon complex<sup>20</sup>. Interactions between the codon-anticodon duplex and the 30S particle induce a folding process between the ribosome and the ternary complex that is consistent with an induced-fit<sup>17</sup> or 'domain closure'<sup>41</sup> mechanism. A comparison of the rates of dissociation of cognate and near-cognate tRNAs from the 0.35 FRET state ( $6.4 \text{ s}^{-1}$  versus  $16.2 \text{ s}^{-1}$ ) indicates that early recognition events preferentially stabilize cognate tRNAs on the ribosome.

Formation of the 0.35 FRET state also allows further movement of the tRNA in the ribosome. The difference in the rates of the reaction  $k_{0.35 \rightarrow 0.5}$  between cognate and near-cognate tRNAs ( $11.8 \text{ s}^{-1}$  versus  $2 \text{ s}^{-1}$ , respectively) suggests that the induced fit moves cognate tRNA into a position better than that of near-cognate tRNA to allow formation of the additional stabilizing contacts with the ribosome that are associated with the 0.5 FRET state where GTP is hydrolyzed.

The time required for a 30S folding reaction such as domain closure is probably much faster than 84 ms (1/11.8 s). Thus, the observed delay in reaching the GTPase-activated state is due to a kinetic barrier, such as a large thermal fluctuation in the position of the tRNA or larger conformational rearrangements of the ribosome, or both. Slight differences in positioning between cognate and near-cognate tRNA owing to interactions with the ribosome could lead to exponentially different probabilities in surmounting this kinetic barrier. This proposal can be tested by obtaining higher time-resolution FRET data and observing whether slight differences in cognate and near-cognate FRET values are found before formation of the 0.5 FRET state. Thus, the same induced-fit mechanism in initial selection gives rise to two selection effects: differences between cognate and near-cognate thermal dissociation and their ability to overcome the kinetic barrier needed to stabilize tRNA-ribosome interactions.

Recent cryo-EM structures of kirromycin-stalled ternary complex on the ribosome (stalled accommodation after GTP hydrolysis) show that EF-Tu contacts the SRL and helix 5 of the small subunit, whereas the aa-tRNA contacts helices 43 and 69 of the large subunit as well as ribosomal protein S12 and perhaps L11 (refs. 24,37). We speculate that the formation of these contacts leads to the stability of the 0.5 FRET state.

The motion of aa-tRNA in the 0.35  $\rightarrow$  0.5 FRET transition provides a mechanistic explanation of the allosteric interaction between codon recognition and GTP hydrolysis. Consider the following observations: (i) codon recognition and the resultant folding of the 30S subunit leads to preferential stabilization of the cognate ternary complex; (ii) the P- to A-site tRNA distance in the kirromycin-stalled ribosome complex is consistent with our 0.5 FRET state; and (iii) EF-Tu is in direct contact with the SRL near the GTP-binding site in the GTPase-activated state<sup>24,37</sup>. From these observations, we infer that the stabilizing contacts in the 0.5 FRET state that end the initial selection process are precisely the contacts needed for GTP activation and hydrolysis.

In this view, the SRL functions as a *trans*-acting, GTPase-activating factor that cannot productively contact EF-Tu until the ternary complex is positioned in the GTPase-activated state (0.5 FRET). This model explains the approximately ten-fold difference in the rates of GTPase activation and GTP hydrolysis observed for cognate and near-cognate aa-tRNAs<sup>17</sup>. In our model, movement of ternary complex into the GTPase-activated state (0.5 FRET) can be achieved only after a kinetic barrier is overcome through conformational changes within the ribosome and thermal fluctuations in the position of tRNA. Increased  $\text{Mg}^{2+}$  concentration likely stabilized

t-RNA-ribosome interactions, as well as increasing the intrinsic rate of GTP hydrolysis, explaining the high sensitivity of GTP hydrolysis to  $Mg^{2+}$  concentration<sup>17</sup>.

In agreement with this model, we observe that specific cleavage of the SRL stalls aa-tRNA selection in the GTPase-activated 0.5 FRET state while not affecting earlier steps in the pathway (see Fig. 2c,e). Ribosomes bearing mutations in the SRL show diminished levels of GTP hydrolysis and hyperaccurate tRNA selection<sup>35</sup>. Mutation and cleavage of the SRL probably modifies its interaction with EF-Tu, slowing its capacity to stimulate GTP hydrolysis. By increasing the delay time in the GTPase-activated state prior to GTP hydrolysis fidelity could be enhanced by allowing additional time for near-cognate ternary complexes to dissociate nonproductively.

The overall fidelity ( $7.1 \times 10^{-3}$ ) of aa-tRNA selection in our system (at 15 mM  $Mg^{2+}$ ) is similar to previous *in vivo* estimates of translational fidelity<sup>12</sup>. Quantitative treatment of the smFRET data shows that there is an ~6-fold selection against near-cognate aa-tRNA during initial selection and ~24-fold selection in proofreading after GTP hydrolysis. As was seen in recent work, we expect that lowering the  $Mg^{2+}$  concentration will further enhance fidelity where initial selection is expected to be most affected<sup>6,17,42</sup>.

Proofreading after GTP hydrolysis arises from the slow rate at which accommodation at the PTC occurs<sup>38</sup>. After GTP hydrolysis, contacts between the aa-tRNA and EF-Tu-GDP are weakened<sup>43</sup>. Release of the 3' end of the aa-tRNA from EF-Tu allows for diffusion into the PTC (Fig. 3, steps 5 and 6). Once freed from its interactions with EF-Tu, the aa-tRNA is only weakly bound to the ribosome, and interactions in the codon-anticodon complex again determine the efficiencies of progression in accommodation.

Our data support previous proposals that induced fit is again used after GTP hydrolysis<sup>17</sup> and that the mechanism may be driven by folding events on the 30S subunit<sup>41</sup>. In keeping with our proposal that codon recognition triggers an initial folding step that positions cognate aa-tRNA closer to the GTPase-activated state, where it can form stabilizing contacts, cognate tRNA may, after breaking its contacts with EF-Tu, again be positioned better than near-cognate tRNA to accommodate at the PTC.

aa-tRNAs make transient fluctuations to a 0.75 FRET state in the GTPase-activated state, both before and after GTP hydrolysis (Fig. 1c,d). This observation suggests that, before EF-Tu converts to the GDP-bound form, the aa-tRNA can sample the accommodated state but not participate in peptide bond formation. GTP hydrolysis and the subsequent conversion of EF-Tu to the GDP-bound conformation may induce a conformational change of the PTC required for complete accommodation and efficient peptide bond formation, as suggested by mutation data and conformational flexibility of the PTC<sup>44–46</sup>. We speculate that the conformational change of EF-Tu may influence peptide bond formation through its interaction with the SRL. This RNA element is physically coupled to the PTC via tertiary interactions with helix 91/92 (refs. 47,48). Specifically, the binding site for the 3' end of the aa-tRNA (the A loop) may be altered by GTP hydrolysis so as to allow efficient accommodation into the PTC.

The results presented here show the efficacy of single-molecule fluorescence for unraveling the dynamic and mechanistic details of translation. aa-tRNA delivery at the A site of the ribosome mediated by EF-Tu is observed to proceed through codon recognition (0.35 FRET) and GTPase-activated (0.5 FRET) intermediates before complete accommodation (0.75 FRET). Fidelity in translation is achieved using both kinetic and steric mechanisms in initial selection before, and proofreading after, GTP hydrolysis. In both of these steps, fidelity is greatly enhanced by differences in the movement of

cognate and near-cognate tRNA promoted by codon-anticodon interactions on the 30S subunit to favor the formation of stabilizing contacts with the 50S subunit. Although it is not known how aa-tRNA selection affects the global conformation of the ribosome, future single-molecule experiments may provide a means of measuring the nature and time scales of ribosomal and tRNA conformational changes required for tRNA selection. Finally, single-molecule experiments provide a direct observation of antibiotic action on the ribosome.

## METHODS

**Reagent preparation and purification.** Tightly coupled *E. coli* 70S ribosomes as well as initiation and elongation factors were purified using standard methods<sup>26</sup>. tRNA<sup>fMet</sup> and tRNA<sup>Phe</sup> and were purchased from Sigma and labeled with Cy3 and Cy5, respectively, at the naturally occurring modified nucleotides acp<sup>3</sup>U at position 47 (tRNA<sup>Phe</sup>) and s<sup>4</sup>U at position 8 (tRNA<sup>fMet</sup>)<sup>26</sup>. Before purification<sup>26</sup>, these tRNAs were aminoacylated, and tRNA<sup>fMet</sup>(Cy3-s<sup>4</sup>U8) was formylated. The ternary complex of EF-Tu-GTP and Phe-tRNA<sup>Phe</sup>(Cy5-acp<sup>3</sup>U47) was prepared as described<sup>26</sup>. Quartz microscope slides for total-internal-reflection (TIR) fluorescence microscopy were prepared as described<sup>26</sup>. Further details of reagent preparation and purification are presented in the **Supplementary Methods** online.

70S ribosomal complexes containing fMet-tRNA<sup>fMet</sup>(Cy3-s<sup>4</sup>U8) in the P site were formed using synthetic 5'-biotinylated mRNAs that contained a 25-nucleotide spacer region, a strong (UAAGGA) Shine-Dalgarno ribosomal binding site and 12 codons derived from the open reading frame of T4 gene product 32. Various 70S complexes were prepared in which only the sequence identity of the second codon was altered from UUU (cognate) to either CUU (near-cognate) or AAA (noncognate). Complexes were purified and immobilized on quartz surfaces as described<sup>26</sup>. Further details about ribosomal complex formation and purification are in **Supplementary Methods** online.

**Single-molecule experiments.** All single-molecule experiments were conducted in the following Tris-polymix buffer system: 50 mM Tris-OAc, pH 7.5 (25 °C), 100 mM KCl, 5 mM NH<sub>4</sub>OAc, 0.5 mM Ca(OAc)<sub>2</sub>, 15 mM Mg(OAc)<sub>2</sub>, 6 mM β-mercaptoethanol, 5 mM putrescine and 1 mM spermidine. To extend the lifetimes and reduce the noise of Cy3 and Cy5 fluorescence, an oxygen-scavenging system composed of 1% (v/v) β-D-glucose, 25 U ml<sup>-1</sup> glucose oxidase and 250 U ml<sup>-1</sup> catalase was used in all experiments as described<sup>26</sup>. A laboratory-built, prism-based TIR apparatus, based on an inverted microscope, was used. Cy3- or Cy5-labeled molecules were excited using a diode-pumped 532-nm laser (CrystalLaser) or a 635-nm diode (Hitachi) laser. Fluorescence emission was collected by a 1.2 NA 60× water-immersion objective (PlanApo, Nikon) and imaged onto a cooled, back-illuminated charge-coupled device (CCD) camera (MicroMax, Roper Scientific) with 9-pixel binning at 100-ms exposure time. Stopped-flow delivery was achieved using a custom-built, motor-driven syringe injection system, where the dead time for complete mixing after delivery of substrates is estimated at ~500 ms. Ternary complex was formed as described<sup>26</sup> at a concentration of 2 μM, diluted with Tris-polymix buffer to a final concentration of 7.5 nM and immediately delivered by stopped flow to surface-immobilized ribosome complexes. Additional details concerning single-molecule experiments as well as the statistical analysis of the data are in **Supplementary Methods** online.

*Note: Supplementary information is available on the Nature Structural & Molecular Biology website.*

## ACKNOWLEDGMENTS

S.C.B. is supported by the Giannini Family Foundation, and R.L.G. is supported by the American Cancer Society. Restrictocin was a gift of C. Correll (University of Chicago). This work was supported by grants to J.D.P. from the US National Institutes of Health (GM51266) and the David and Lucille Packard Foundation, to S.C. from the US National Science Foundation, the US National Aeronautics and Space Administration and the US Air Force Office of Scientific Research, and to S.C. and J.D.P. from the David and Lucille Packard Foundation Interdisciplinary Science Program (grant 2000-01671). The authors thank E. Lau for technical support, J. Hoch for suggestions relating to fluorescence quenching, E.V. Puglisi for

critical discussions and scientific input, and M. Dorywalska and J. Choy for comments on the written manuscript.

## COMPETING INTERESTS STATEMENT

The authors declare that they have no competing financial interests.

Received 16 April; accepted 10 August 2004

Published online at <http://www.nature.com/nsmb/>

1. Ramakrishnan, V. Ribosome structure and the mechanism of translation. *Cell* **108**, 557–572 (2002).
2. Hazlett, T.L., Johnson, A.E. & Jameson, D.M. Time-resolved fluorescence studies on the ternary complex formed between bacterial elongation factor Tu, guanosine 5'-triphosphate, and phenylalanyl-tRNA<sup>Phe</sup>. *Biochemistry* **28**, 4109–4117 (1989).
3. Gavrilova, L.P., Perminova, I.N. & Spirin, A.S. Elongation factor Tu can reduce translation errors in poly(U)-directed cell-free systems. *J. Mol. Biol.* **149**, 69–78 (1981).
4. Gavrilova, L.P., Kostiyashkina, O.E., Koteliansky, V.E., Rutkevitch, N.M. & Spirin, A.S. Factor-free ("non-enzymic") and factor-dependent systems of translation of polyuridylic acid by *Escherichia coli* ribosomes. *J. Mol. Biol.* **101**, 537–552 (1976).
5. Rodnina, M.V. & Wintermeyer, W. Ribosome fidelity: tRNA discrimination, proofreading and induced fit. *Trends Biochem. Sci.* **26**, 124–130 (2001).
6. Gromadski, K.B. & Rodnina, M.V. Kinetic determinants of high-fidelity tRNA discrimination on the ribosome. *Mol. Cell* **13**, 191–200 (2004).
7. Hamel, E., Koka, M. & Nakamoto, T. Requirement of an *Escherichia coli* 50S ribosomal protein component for effective interaction of the ribosome with T and G factors and with guanosine triphosphate. *J. Biol. Chem.* **247**, 805–814 (1972).
8. Lijias, A. & Gudkov, A.T. The structure and dynamics of ribosomal protein L12. *Biochimie* **69**, 1043–1047 (1987).
9. Rodnina, M.V. & Wintermeyer, W. Fidelity of aminoacyl-tRNA selection on the ribosome: kinetic and structural mechanisms. *Annu. Rev. Biochem.* **70**, 415–435 (2001).
10. Rodnina, M.V. *et al.* GTPases mechanisms and functions of translation factors on the ribosome (Review). *Biol. Chem.* **381**, 377–387 (2000).
11. Gale, E.F., Cundliffe, E., Reynolds, P.E., Richmond, M.H. & Waring, M.J. *The Molecular Basis of Antibiotic Action* (Wiley, London, 1981).
12. Parker, J. Errors and alternatives in reading the universal genetic code. *Microbiol. Rev.* **53**, 273–298 (1989).
13. Grosjean, H.J., Henau, S. & Crothers, D.M. On the physical basis for ambiguity in genetic coding interactions. *Proc. Natl. Acad. Sci. USA* **75**, 610–614 (1978).
14. Hopfield, J.J. Kinetic proofreading: a new mechanism for reducing errors in biosynthetic processes requiring high specificity. *Proc. Natl. Acad. Sci. USA* **71**, 4135–4139 (1974).
15. Ninio, J. Kinetic amplification of enzyme discrimination. *Biochimie* **57**, 587–595 (1975).
16. Thompson, R.C. & Dix, D.B. Accuracy in protein synthesis. A kinetic study of the reaction of poly(U)-programmed ribosomes with a leucyl-tRNA<sub>2</sub> elongation factor Tu-GTP complex. *J. Biol. Chem.* **257**, 6677–6682 (1982).
17. Pape, T., Wintermeyer, W. & Rodina, M.V. Induced fit in initial selection and proofreading of aminoacyl-tRNA on the ribosome. *Eur. J. Mol. Biol.* **18**, 3800–3807 (1999).
18. Fourmy, D., Recht, M.I., Blanchard, S.C. & Puglisi, J.D. Structure of the A site of *E. coli* 16S ribosomal RNA complexed with an aminoglycoside antibiotic. *Science* **274**, 1367–1371 (1996).
19. Yoshizawa, S., Fourmy, D. & Puglisi, J.D. Recognition of the codon-anticodon helix by ribosomal RNA. *Science* **285**, 1722–1725 (1999).
20. Ogle, J.M. *et al.* Recognition of cognate transfer RNA by the 30S ribosomal subunit. *Science* **292**, 897–902 (2001).
21. Ogle, J.M., Carter, A.P. & Ramakrishnan, V. Insights into the decoding mechanism from recent ribosome structures. *Trends Biochem. Sci.* **28**, 259–266 (2003).
22. Piepenburg, O. *et al.* Intact aminoacyl-tRNA is required to trigger GTP hydrolysis by elongation factor Tu on the ribosome. *Biochemistry* **39**, 1734–1738 (2000).
23. Powers, T. & Noller, H.F. The 530 loop of 16S rRNA: a signal to EF-Tu? *Trends Genet.* **10**, 27–31 (1994).
24. Valle, M. *et al.* Incorporation of aminoacyl-tRNA into the ribosome as seen by cryo-electron microscopy. *Nat. Struct. Biol.* **10**, 899–906 (2003).
25. Watson, B.S. *et al.* Macromolecular arrangement in the aminoacyl-tRNA elongation factor Tu-GTP ternary complex. A fluorescence energy transfer study. *Biochemistry* **34**, 7904–7912 (1995).
26. Blanchard, S.C., Kim, H.D., Gonzalez, R.L. Jr., Puglisi, J.D. & Chu, S. tRNA dynamics on the ribosome during translation. *Proc. Natl. Acad. Sci. USA* **101**, 12893–12898 (2004).
27. Plumbridge, J.A., Baumert, H.G., Ehrenberg, M. & Rigler, R. Characterisation of a new, fully active fluorescent derivative of *E. coli* tRNA<sup>Phe</sup>. *Nucleic Acids Res.* **8**, 827–843 (1980).
28. Cundliffe, E. Antibiotics and prokaryotic ribosomes: action interaction and resistance. In *Ribosomes, Structure, Function, and Genetics*. Proceedings of the 9<sup>th</sup> Steenbock Symposium (eds. Chambliss, G. *et al.*) 555–581 (University Park Press, Baltimore, 1980).
29. Rodnina, M.V., Fricke, R. & Wintermeyer, W. Transient conformational states of aminoacyl-tRNA during ribosome binding catalyzed by elongation factor Tu. *Biochemistry* **33**, 12267–12275 (1994).
30. Vozeley, L., Palm, G.J., Mesters, J.R. & Hilgenfeld, R. Conformational change of elongation factor Tu (EF-Tu) induced by antibiotic binding. Crystal structure of the complex between EF-Tu.GDP and aureodox. *J. Biol. Chem.* **276**, 17149–17155 (2001).
31. Wolf, H., Chinali, G. & Parmeggiani, A. Mechanism of the inhibition of protein synthesis by kirromycin. *Eur. J. Biochem.* **75**, 67–75 (1977).
32. Moazed, D., Robertson, J.M. & Noller, H.F. Interaction of elongation factors EF-G and EF-Tu with a conserved loop in 23S RNA. *Nature* **334**, 362–364 (1988).
33. Hausner, T.P., Atmadja, J. & Nierhaus, K.H. Evidence that the G2661 region of 23S rRNA is located at the ribosomal binding sites of both elongation factors. *Biochimie* **69**, 911–923 (1987).
34. Kurland, C.G., Hughes, D. & Ehrenberg, M. *Limitations of Translational Accuracy* 979–1004 (American Society for Microbiology Press, Washington, DC, 1996).
35. Bilgin, N. & Ehrenberg, M. Mutations in 23S ribosomal RNA perturb transfer RNA selection and can lead to streptomycin dependence. *J. Mol. Biol.* **235**, 813–824 (1994).
36. Valle, M. *et al.* Cryo-EM reveals an active role for aminoacyl-tRNA in the accommodation process. *EMBO J.* **21**, 3557–3567 (2002).
37. Stark, H. *et al.* Ribosome interactions of aminoacyl-tRNA and elongation factor Tu in the codon-recognition complex. *Nat. Struct. Biol.* **9**, 849–854 (2002).
38. Pape, T., Wintermeyer, W. & Rodnina, M.V. Complete kinetic mechanism of elongation factor Tu-dependent binding of aminoacyl-tRNA to the A site of the *E. coli* ribosome. *EMBO J.* **17**, 7490–7497 (1998).
39. Brodersen, D.E. *et al.* The structural basis for the action of the antibiotics tetracycline, pactamycin, and hygromycin B on the 30S ribosomal subunit. *Cell* **103**, 1143–1154 (2000).
40. Gordon, J. Hydrolysis of guanosine 5'-triphosphate associated with binding of aminoacyl transfer ribonucleic acid to ribosomes. *J. Biol. Chem.* **244**, 5680–5686 (1969).
41. Ogle, J.M., Murphy, F.V., Tarry, M.J. & Ramakrishnan, V. Selection of tRNA by the ribosome requires a transition from an open to a closed form. *Cell* **111**, 721–732 (2002).
42. Thompson, R.C., Dix, D.B., Gerson, R.B. & Karim, A.M. Effect of Mg<sup>2+</sup> concentration, polyamines, streptomycin, and mutations in ribosomal proteins on the accuracy of the two-step selection of aminoacyl-tRNAs in protein biosynthesis. *J. Biol. Chem.* **256**, 6676–6681 (1981).
43. Janiak, F. *et al.* Fluorescence characterization of the interaction of various transfer RNA species with elongation factor Tu.GTP: evidence for a new functional role for elongation factor Tu in protein biosynthesis. *Biochemistry* **29**, 4268–4277 (1990).
44. O'Connor, M.O. & Dahlberg, A.E. The involvement of two distinct regions of 23S ribosomal RNA in tRNA selection. *J. Mol. Biol.* **254**, 838–847 (1995).
45. Muth, G.W., Chen, L., Kosek, A.B. & Strobel, S.A. pH-dependent conformational flexibility within the ribosomal peptidyl transferase center. *RNA* **7**, 1403–1415 (2001).
46. Bayfield, M.A., Dahlberg, A.E., Schulmeister, U., Dorner, S. & Barta, A. A conformational change in the ribosomal peptidyl transferase center upon active/inactive transition. *Proc. Natl. Acad. Sci. USA* **98**, 10096–10101 (2001).
47. Harms, J. *et al.* High resolution structure of the large ribosomal subunit from a mesophilic eubacterium. *Cell* **107**, 679–688 (2001).
48. Ban, N., Nissen, P., Hansen, J., Moore, P.B. & Steitz, T.A. The complete atomic structure of the large ribosomal subunit at 2.4 Å resolution. *Science* **289**, 905–920 (2000).